

CHRONIC THORACIC HEMISECTION SPINAL CORD INJURY IN ADULT RATS
INDUCES A PROGRESSIVE DECLINE IN TRANSMISSION FROM UNINJURED FIBERS
TO LUMBAR MOTONEURONS.

Victor L. Arvanian^{1*},

Lisa Schnell²,

Li Lou¹

Roozbeh Golshani³,

Arsen Hunanyan¹,

Ghosh Arko²,

Damien D. Pearse³,

John K. Robinson⁴,

Martin E. Schwab²,

James W. Fawcett⁵

Lorne M. Mendell¹

1 Department of Neurobiology and Behavior

SUNY at Stony Brook, Life Sciences Building,

Stony Brook, NY 11794-5230

2 University of Zurich,

Brain Research Institute, Winterthurerstr 190

CH-8057 Zurich, Switzerland

3 University of Miami Miller School of Medicine, Department of Neurological Surgery, The Neuroscience Program, Miami Project to Cure Paralysis.

4 Department of Psychology

SUNY at Stony Brook,

Stony Brook, NY 11794-5230

5 Cambridge University

Ctr Brain Repair, Robinson Way,

Cambridge CB2 0PY, United Kingdom

* Present Address: Northport Veterans Affairs Medical Center

79 Middleville Road, Bld. 62

Northport, NY 11768

Abstract

Although most spinal cord injuries are anatomically incomplete, only limited functional recovery has been observed in people and rats with partial lesions. To address why surviving fibers cannot mediate more complete recovery, we evaluated the physiological and anatomical status of spared fibers after unilateral hemisection (HX) of thoracic spinal cord in adult rats. We made intracellular and extracellular recordings at L5 (below HX) in response to electrical stimulation of contralateral white matter above (T6) and below (L1) HX. Responses from T6 displayed reduced amplitude, increased latency and elevated stimulus threshold in the fibers across from HX, beginning 1-2 weeks after HX. Ultrastructural analysis revealed demyelination of intact axons contralateral to the HX, with a time course similar to the conduction changes. Behavioral studies indicated partial recovery which arrested when conduction deficits began. These findings suggest a chronic pathological state in intact fibers and necessity for prompt treatment to minimize it.

Most spinal cord injuries (SCI; ~ 90%) are anatomically incomplete, with spared fibers spanning the damaged spinal segments. However, almost 50% of all spinal cord injuries are functionally complete, with total loss of sensation and muscle control below the level of the injury (1-4). Therefore we hypothesize that some of the surviving fibers might not conduct or that their synaptic action is too weak to elicit functional effects.

As a model of incomplete injury we used lateral left spinal hemisection (HX), with the right side of the spinal cord remaining intact. This model allows the study and comparison of how acute and chronic trauma affect the function of the surviving ventrolateral funiculus (VLF) fibers. The VLF contains ascending and descending fibers that are known to play an important role in a variety of sensory and motor functions, including somatosensory function, locomotion, bladder function and ejaculation (reviewed in 5-11). Although a variable fraction of VLF fibers in the white matter tracts survive most SCI, it is not clear whether these surviving fibers can affect sensory relay nuclei above the injury or motoneurons below the injury, and whether transmission remains constant during the chronic phase after injury.

To study the time-related changes in transmission across the hemisection, we measured the intracellular synaptic response in lumbar L5 MNs on both the left (lesioned) or right (intact) sides, evoked by electrical stimulation of the ipsilateral or contralateral VLF at T6 (above the HX), and/or at L1 (below the HX). In the same cords, a tungsten electrode was placed into the right ventral horn to record evoked potentials extracellularly. These responses were compared in intact rats and at different time points after the HX, i.e., immediately, after 2 days, 1 week and up to 14 weeks. Prior to the terminal electrophysiological recordings, locomotor function of the rats

was assessed in the Open Field, Irregular Horizontal Ladder and Narrowing Beam behavioral tests. After completion of electrophysiological recordings, the cords were processed to compare transmission across the HX with the anatomical measures, such as (i) severity of the injury (anatomical reconstruction), and (ii) the degree of myelination and numbers of axons on the uninjured side of the cord using light and electron microscopy, as well as (iii) immunolabeling with antibody for Neurofilament-H (NF-H, axonal marker).

Our studies reveal a decline in function of white matter across from the hemisection beginning about 1 week after injury. This was associated with demyelination of axons within that region and decreased locomotor function in challenging behavioral tasks. Some of these findings have been reported in abstract form (12-14).

Methods.

Spinal cord injury and all experimental procedures were performed in accordance with protocols approved by the Institutional Animal Care and Use Committee at SUNY- Stony Brook.

Surgical procedure for the hemisection lesion. Adult (~210 g) female Sprague-Dawley rats were deeply anesthetized in 3% isoflurane in 100% O₂ in an induction chamber (1L). Anesthesia was maintained by administering 1.5% isoflurane in 100% O₂ through a face mask. Rectal temperature was maintained at 36°C via a heating pad and heart rate was monitored throughout the procedure. Dorsal laminectomy was performed to expose segments T9-T11 of the spinal cord. The dura was slit (1 mm) at the midline at T10. A complete hemisection of the left hemicord at T10 was carried out with the tip of iridectomy scissors, as follows: first, while

holding the dura and lifting the spinal cord slightly, one tip of the scissors was passed through the entire thickness of the spinal cord dorsal to ventral at the midline; the left dorsal and ventral columns were then cut from lateral to the midline by closing other tip of scissors; finally, while keeping the cord elevated, one tip of the scissors was placed under the ventral surface of the spinal cord (up to the midline) and any uncut tissue in the left dorsal and ventral columns was cut ventral to dorsal up to the midline. After surgery, the muscles and skin were closed in layers with 4-0 suture. Antibiotic (Baytril, 5mg/kg, 0.1 ml sc), analgesic (Buprenorphine 5mg/kg, 0.1 ml sc), and 10 cc of sterile saline were administered subcutaneously. Bladder function was not compromised by this surgery.

Behavioral assessment (see Fig. 5) and criteria for animals exclusion. Observation of the freely moving animals in the Open Field (15) has revealed that rats and mice spontaneously recover weight-bearing stepping in the hind limb ipsilateral to lateral hemisection of the cervical or thoracic spinal cord (16-18). However, severe deficits with no recovery after unilateral hemisection of the cervical spinal cord were observed in more challenging tests, such as Narrowing Beam and Horizontal Rope (Ladder) tests, which measure primarily motor function (19). Therefore, in order to examine the locomotor function after lateral hemisection injury, the traditional Open Field BBB score (15) was supplemented with the more challenging Irregular Horizontal Ladder and Narrowing Beam tests (19, 20). Animals were pre-trained for 4 weeks before the surgery for these tests, which were carried out at weekly intervals for up to 6 weeks after surgery using following protocols:

BBB scoring: Rats were allowed to move freely and scored during a 4 minute period for their ability to use their hindlimbs by two independent blinded observers. Joint movements, paw

placement, weight support, and fore/hindlimb coordination were judged according to the 21-point BBB locomotion scale.

Narrowing Beam Crossing: Rats were trained to cross the elevated progressively narrowing beam starting from the widest side. Two independent investigators marked the unit (50 mm apart) when the first slip occurred during five runs. The trained non-injured rats completed the course with no slip or at most very few. Hemisection severely affected ability of rats to perform this challenging test. The first slip of either limb was scored because slips occurred randomly and in most cases the slip of one hindlimb followed by an immediate slip of the other hindlimb.

Horizontal Irregular Ladder Crossing test: The animals were trained to run across a 1-meter-long horizontal ladder elevated from the ground. A 60 cm stretch was chosen for filming and analysis. To prevent habituation to a fixed bar distance, we placed the bars irregularly (1-4cm spacing). The number of foot slips or total misses in three trials was counted by two independent investigators and normalized by the total number of steps.

In addition to these tests, rats were observed in the Open Field at day 1 post-surgery (to evaluate the level of injury), and BBB scoring was carried at days 2 and 4 and then at weekly intervals for 6 weeks. Open field observations are particularly important after the initial days post-HX when rats cannot perform the more challenging tests.

Some animals were excluded from the study according to the following criteria: (i) rats showing weight-bearing stepping in the hind limb ipsilateral to the injury at day 1 post-HX indicating that the hemisection was not complete (1 rat of 105); (ii) animals not gaining weight, showing signs of autotomy, developing skin lesions or ruffled fur, squealing in response to gentle handling,

licking a particular spot, or vocalizing were interpreted as suffering pain. These rats were sacrificed after evaluation by the attending veterinarian (15 rats of 105).

In vivo intracellular recordings from individual motoneurons (see Fig. 1) and extracellular recordings of the evoked potentials (see Figs. 2, 3) in damaged spinal cord. In the case of acute SCI, the electrophysiological recordings were made initially from the anesthetized (see Fig. 1) non-injured animal. After taking control measurements, the spinal cord was hemisected as above and recordings were made immediately after HX to demonstrate the effect of acute hemisection on the synaptic input to motoneurons from the contralateral white matter at the level of injury. In the case of chronic SCI, animals were allowed to survive for several days/weeks after the initial HX before recordings were made in a terminal procedure.

All rats studied electrophysiologically were deeply anesthetized using a ketamine (80 mg/kg, 0.5 ml) / xylazine (10 mg/kg, 0.5 ml) mixture IP for induction, and 1/5 dose after that, as needed. Heat rate and expired CO₂ were monitored continuously. Dorsal laminectomy of the spinal cord was performed from T5 to T7 and from L1 to L6. A monopolar stimulating tungsten electrode was placed at T6 either on the side of the HX or contralaterally as described in text for VLF stimulation. This electrode entered the cord between the lateral side of the cord and dorsal root entry zone, between the T5-T6 dorsal roots. It was angled 25° from the vertical in the sagittal plane (tip directed caudally), and lowered to a depth of 0.7 mm. Stimulation was also carried out at L1 (see below).

Intracellular recordings from motoneurons (MNs) were made at L5 on either side of the cord using sharp glass microelectrodes (3M KAcetate; 50-70 M Ω resistance), coupled to an Axon Instruments amplifier, digitizer, and a PC. Motoneurons were identified by their antidromic response to stimulation of the cut L5 ventral root. The resting membrane potential of motoneurons used for analysis ranged from -45 to -65 mV. In addition, a tungsten electrode was used to record composite evoked potentials extracellularly from the L5 ventral horn contralateral to the HX. It was positioned to enter the right side of the cord at the dorsal root entry zone, at an angle of 25^o from vertical in the sagittal plane (tip directed rostrally), and was lowered to a depth of 1.3 mm. These recordings were amplified, digitized and stored on a PC. The amplitude of the maximum response was measured using an average of 200 consecutive responses. All records were analyzed off line using PClamp 9.0.

Synaptic responses on both sides of the cord were evoked by electrical stimulation VLF at T6 (rostral to the HX) both ipsilateral and contralateral to the HX. These recordings were made to detect the functional connections from axons passing through the injured region. If VLF stimulation above the injury level failed to evoke a response in L5 MNs, we moved the stimulating electrode caudal to the HX and recorded responses at L5 evoked by stimulation of VLF at L1. In many cases we managed to record responses evoked by stimulation of VLF rostral and caudal to HX in the same motoneuron. The VLF stimulus had a duration of 50 μ s and was delivered at 1 Hz. The intensity was chosen to evoke a maximum response. It usually ranged from 40-70 μ A for the ipsilateral stimulus and 120-270 μ A for contralateral stimulus in uninjured cords, and 400-700 μ A from contralateral VLF in hemisectioned cords. The threshold and

the maximum stimulation currents were determined by examining responses to currents of increasing intensity.

Responses from all motoneurons for a given stimulus were averaged over all motoneurons recorded in each rat. These average values were compared over all animals in a given condition, i.e. the degrees of freedom are derived from the number of animals, not the total number of cells. Data were compared first by carrying out one-way ANOVA (Sigmastat 2.0). If significant differences were observed between the groups, a Student-Newman-Keuls test was used for pairwise multiple comparisons between them.

Histology to determine extent of the injury After completion of electrophysiological recording the rats were intracardially perfused and spinal cords prepared for morphological evaluation of the injury site. A 1-cm segment of cord at the lesion zone was cut on a cryostat at 10 μm , and the Cresyl Violet stained sections were viewed using a Zeiss Axioskop upright microscope. Images were captured using a Spot RT camera and ImagePro Plus software (Media Cybernetics, Inc.) and used for reconstructions of the injury site, as previously described (20, 21; see Fig. 1).

Immunohistochemistry experiments using NF-H antibody to label axons in the white matter across from HX. Rats of 4 groups, i.e. immediately post-HX and 2 days, 1 week and 6 weeks post-HX (3 rats per group), were re-anesthetized (urethane, 2g/kg i.p.), transcardially perfused and horizontal sections of the spinal cord (20 μm) were processed for Neurofilament NF-H immunolabeling (described in (22-23)). Cryosections were incubated in a humidity chamber for 1 h in 0.1M PBS containing 0.4% Triton X-100 with .1:30 Goat serum (GS-PBS-T; to block

nonspecific binding), incubated in 1:2000 rabbit-anti-Neurofilament-H (Novus Biologicals, Inc) overnight, rinsed and then incubated with 1:100 AlexaFluor 594 goat-anti-rabbit IgG (Molecular Probes) for 3 hours. After three rinses, the sections were coverslipped with Prolong Gold antifade reagent (Molecular Probes) and viewed using a Zeiss Axioskop upright microscope with appropriate fluorescence bandpass filter. Images were captured from consecutive sections ventral-to-dorsal using a Spot RT camera with ImagePro Plus software (Media Cybernetics) within 48 h of completing the staining procedures. The immunolabeling signal was examined at 100x magnification in the white matter contralateral to HX (see Supplementary Fig. 1).

Estimation of myelinated and total axon counts. Plastic embedding of a 2-mm-long piece of the fixed spinal cord at the lesion epicenter was prepared as described previously (24, 25). Total numbers of myelinated axons in the VLF region were counted using computer-assisted microscopy and Stereoinvestigator software (MicroBrightfield) in three 1 μ m plastic toluidine-blue stained semi-thin transverse sections taken from the tissue block. The three numbers were then averaged for a final estimate. For myelinated/unmyelinated axon ratios in the VLF, thin sections from the tissue block were examined and photographed using a Philips CM10 electron microscope. Total fiber number was calculated by multiplying myelinated axon count and ratio of unmyelinated to myelinated axons and adding the resulting number to the myelinated axon count.

Results

VLF to motoneuron connections in normal animals.

In uninjured rats, stimulation of the left VLF at T6 evoked responses in ipsilateral L5 motoneurons averaging 5.8 ± 0.9 mV (n=14) in peak amplitude and 1.4 ± 0.2 ms in latency (i.e. measured from stimulus artifact to response onset) (Fig. 1). Stimulation of the contralateral right VLF at T6 evoked a synaptic response in the same motoneurons, but these responses exhibited a somewhat smaller peak amplitude (2.8 ± 0.3 mV, n = 14) and markedly longer latency (6.0 ± 0.7 ms). The difference in latency of the response from contralateral and ipsilateral VLF was statistically significant ($p < 0.05$, n = 14). Besides differences in latency, the shape of these responses was very different. The short-latency responses from ipsilateral VLF exhibited a brief rise time and consecutive responses (at 1 Hz frequency) were almost identical during the rising phase (see insets in Fig 1ai). In contrast, the longer-latency responses from contralateral VLF had markedly longer rising time-to-peak and showed greater fluctuation rate in both amplitude and latency (see insets in Fig 1bi). The other difference was the significantly higher level of stimulus intensity required to evoke a maximal contralateral response, i.e., 55.2 ± 13.5 μ A for the ipsilateral stimulus and 198.4 ± 27.5 μ A for the contralateral stimulus, respectively ($p < 0.05$, n = 14). The short latency and high reliability of the ipsilateral response suggests that it was almost certainly monosynaptic. The contralateral response is more difficult to characterize. It required much higher stimulus current suggesting the possibility that smaller, slower conducting fibers were responsible, and the long latency suggests that additional synapses were possibly involved in this crossed projection.

VLF to motoneuron connections after spinal cord hemisection.

After measurements of ipsilateral and contralateral responses in uninjured spinal cord, we performed a HX of the left lateral side of the cord while the animal was anesthetized, and the

same responses were examined (Fig. 1-ii). As expected, the monosynaptic response in motoneurons at L5 from stimulating ipsilaterally above the lesion vanished. However, in the same motoneuron the long latency responses following stimulation of the contralateral right VLF at T6 above the HX remained, and the peak amplitude of these responses was not significantly different from that prior to HX (i.e., 2.8 ± 0.7 mV pre-HX vs 2.5 ± 0.5 mV post-HX, $n = 5$, $p > 0.05$).

To investigate the effects of chronic hemisection on these connections, hemisected rats were allowed to survive for up to 14 weeks, and electrophysiological recordings were carried out in terminal experiments at 2 days, 1 week, 2 weeks and 3- to - 14 weeks post-HX. The response in L5 motoneurons from contralateral T6 VLF stimulation was unaffected 2 days post-HX. However, beginning 1 week post-HX, this response declined and was markedly diminished by 2 weeks post-HX, even when high (up to 700 μ A) intensity stimuli were applied (Fig. 1-iii). Furthermore, the responses remained diminished for the remainder of the 14 weeks post-HX that was investigated. While transmission from VLF rostral to the HX remained depressed, motoneurons still received inputs from the ipsilateral VLF caudal to HX, although these responses became somewhat smaller in amplitude in comparison to with non-injured ipsilateral controls (trace C-iii in Fig. 1). No change in latency was observed in these ipsilateral projections caudal to Hx. A summary of these results is presented in Fig. 1f. These results suggest that there was a failure of conduction of the contralateral VLF through the segment of injury, which started to develop 1 week after the HX.

After completion of the electrophysiological recordings all rats were perfused, and cross-sections were processed to evaluate the extent of the HX by digital reconstruction (Fig. 1e). We found that injuries were uniform, with complete lesion of the left half of the cord. There was no correlation between the size of the lesioned area and the transmission from the contralateral VLF to ipsilateral motoneurons at the different times after HX (not shown).

Conduction in the VLF contralateral to the lesion side: extracellular recordings.

The results in the previous paragraph suggested that there might be a delayed conduction deficit developing in unlesioned VLF axons contralateral to the injury. We tested this hypothesis first by recording extracellularly from VLF axons in response to stimulation above and below the lesion level (Fig. 2). In the uninjured spinal cord, electrical stimulation of the right VLF at T6 (ipsilateral to tungsten recording electrode) usually evoked a response that consisted of 2 or 3 peaks. We confirmed the neural basis of these waves by demonstrating their invariance in response to changing stimulus polarity (Fig. 2). Furthermore, at a stimulus frequency of 1 Hz we observed a marked fluctuation in both amplitude and latency in up-going waves (ii) and (iii), but not in the shortest-latency up-going wave (i). These fluctuations (waves ii and iii only) were even more apparent when the stimulation frequency was raised to 10 Hz (not shown). This and measurements of latencies suggests that wave (i) represents the volley of action potentials in white matter axons, while waves (ii) and (iii) represent synaptic responses (Fig. 2). These peaks (i-iii) were preserved immediately after left HX with no significant changes in amplitude ($p > 0.05$, $n = 7$, Fig. 2). Further investigation revealed that all peaks were preserved even after transection of 2/3 of the cord ($n = 3$, Fig. 2), but were eliminated after complete transection ($n = 4$, Fig. 2).

In order to compare the ability of VLF to transmit through the intact side from above the hemisection to below, we measured the maximum amplitude of the volleys and synaptic response recorded in L5 in response to stimulation at T6 in intact (uninjured) preparations, after acute hemisection (Fig. 2), and after chronic hemisection (Fig. 3). In the same preparations we also recorded the stimulus intensity required to obtain a threshold response and the maximum response. We measured the amplitude of the extracellularly recorded evoked potentials as the voltage difference between the deepest trough to the positive peak of the first wave response (volley of action potentials, generally at 0.5-1 ms) and the last wave response (synaptic, generally at 3-5 ms). The results are displayed in Table 1 where it is shown that there were no differences between the amplitude of the synaptic responses obtained after acute hemisection (compared to the intact) but after chronic hemisection, the responses were smaller and required greater stimulus intensity to obtain them. In addition, the action potential volleys conducted across the segment contralateral to HX were also substantially reduced after chronic hemisection (Table 1). The diminished responses across the injury in chronically hemisected rats could not be enhanced by repositioning either the recording or stimulating electrode by as much as 0.5 mm rostrocaudal and/or mediolateral, indicating that the decline was not the result of the location of the electrodes, but rather was the result of diminished conduction/ transmission across the HX. These results indicate that fibers passing through the region across from the HX underwent a change in their properties beginning about 1 -2 weeks after HX.

Intracellular recordings from motoneurons.

Consistent with these extracellular recording results, intracellular recordings from motoneurons contralateral and caudal to HX revealed marked change in synaptic responses evoked by stimulation of VLF on the intact side of the spinal cord rostral to the level of the chronic HX (Fig. 3; Table 2- compare rows 1 and 2). The responses exhibited a decline in amplitude, an increase in latency and an increase in the stimulus intensity required to elicit the maximum response ($p < 0.05$, One Way ANOVA). In these experiments we also systematically determined the same parameters in response to stimulation at L1, caudal to HX. As observed in Table 2 (see also Fig. 3) these responses after chronic HX were similar to those observed in the intact spinal cord. The difference in latency of synaptic responses evoked from above and below T10 permitted an estimate of conduction velocity of fibers crossing this segment. It averaged in 39 ± 5 m/s ($n = 7$) in uninjured cords and 22 ± 4 m/s ($n = 10$) in chronically hemisected cords ($p < 0.05$). These findings suggest that fibers passing directly across from the HX were affected by the HX but that a population of propriospinal fibers in lumbar cord were normal in their properties despite T10 HX.

Neurofilament-H (NF-H) immunolabeling.

To study if the striking decline of axonal conduction might be associated with the loss of axons in contralateral to chronic HX white matter, we used the NF-H antibody to mark the axons in horizontal sections across from HX in the region of the VLF. The NF-H antibody has been widely utilized for detection of axons in the damaged spinal cord, regardless of whether these axons are functional (22, 23). Qualitative analysis of NF-H immunohistochemical staining images, within the vicinity of the HX, yielded no noticeable difference between the following groups: 10 minutes, 2 days, 1 week, 2 weeks and 6 weeks post-HX (3 to 6 rats per time point)

(Supplementary Fig. 1). These observations suggest that fibers in the contralateral white matter across from the HX are largely spared. We therefore performed a more detailed analysis of axon numbers and myelination.

Estimation of myelinated and total axon counts in the region of the VLF.

We used light and electron microscopy to investigate quantitatively whether the decay of transmission and decrease in conduction velocity following chronic HX was due to a decrease in either total axon number or the number of myelinated axons within the white matter contralateral to the HX. After completion of electrophysiological recordings, animals were perfused and spinal cords prepared for morphological evaluation at different time points post-injury: 10 min post-HX (acute injury) and 2- or 6- weeks post-HX (chronic injury; 4 rats in each group). Tissue specimens were then evaluated for central axon myelination on the right side of the thoracic spinal cord at T10 (the intact side). A decreasing trend was observed in total axon number with the onset of chronic HX ($258,135 \pm 22,335$ acute HX; $194,487 \pm 81,082$ two wks post-HX; $191,766 \pm 25,252$ six wks post-HX), but there was no statistically significant difference between the three groups (one way ANOVA, Kruskal-Wallis test, $p > 0.05$). Importantly, we noted a statistically significant decrease in the number of myelinated axons in the spared white matter in chronic versus acute HX rats (e.g. $99,491 \pm 3,222$ acute HX vs $56,480 \pm 7,094$ two wks post-HX and $62,632 \pm 2,809$ six wks post-HX, $p < 0.05$) (Fig. 4). The percentage of myelinated fibers, calculated as a percent of the total number of axons, was lower in chronically vs acutely HX rats ($38 \pm 3\%$ acute HX, $28 \pm 2\%$ two wks post-HX and $35 \pm 2\%$ six wks post-HX), but these differences were not statistically significant ($p > 0.05$).

Behavioral assessments.

Prior to physiological recordings, rats were pretrained for 4 weeks to perform behavioral tests and locomotor behavior was observed using the open field BBB analyses, the Irregular Horizontal Ladder Crossing test and the Narrowing Beam Crossing test. Scores were taken prior to HX and then at different time points post-HX (Fig. 5). Consistent with previous observations (16-18), spontaneous partial recovery of locomotion of both hindlimbs, ipsilateral and contralateral to HX, occurred during the 2 weeks following lateral HX of the thoracic spinal cord (Fig. 5). In case of the open field BBB analyses, when the rats were not challenged, the degree of locomotor recovery was high and most rats displayed weight-bearing plantar stepping of both hindlimbs, although rotation of the hindlimbs was characteristic for the majority of hemisected rats. In contrast, an obvious and severe impairment was revealed when the rats performed more challenging tasks, e.g. the Irregular Horizontal Ladder Crossing test and the Narrowing Beam Crossing tests (Fig. 5). Importantly, in all three tests the locomotor recovery of both hindlimbs reached a plateau at about 2 weeks post-HX and further recovery did not take place. Interestingly, this time point coincided with the decline of transmission in the contralateral VLF across from the HX.

Discussion

The major finding from this research is that hemisection at T10 reduces transmission from the contralateral white matter above the hemisection to target cells in the lumbar spinal cord. The deficits in conduction/ transmission for fibers running through the segment that had been hemisected contralaterally did not develop immediately after hemisection, but only after 1-2 weeks. They were measured as a marked decline in amplitude of the conducted volleys and

synaptic responses below the segment of HX. In chronically hemisected rats these responses were always subthreshold for action potential generation, which required intracellular recording in order to be measured. The latency of these synaptic responses was increased suggesting a reduction of the conduction velocity of the axons (Figs. 1-3). The electrical threshold to obtain fiber volleys and synaptic responses was elevated by roughly a factor of 10. All of these changes are suggestive of alterations in the properties or composition of the fiber tract spanning the segment opposite the HX. No such changes in electrical threshold and conduction velocity were observed in fibers activated *below* the hemisection (e.g., at L1) although a modest decline in the synaptic potentials in motoneurons was observed from surviving axons ipsilateral to the hemisection. These responses were probably elicited largely by intact ascending and descending propriospinal fibers in the VLF (26-28) extending from L1 to L5 and synapsing with motoneurons (29). Our studies provide little information concerning the mechanism by which this change in conduction occurs. Damage to the cord could result in inflammation (reviewed in 30, 31), release of nitric oxide (reviewed in 32), and other pathological changes resulting in eventual dysfunction of axons contralateral to the injury.

Previous *in vivo* studies using the contusion or compression models (32-35) have revealed similar declines in conduction although the time course is very different. In contrast to the present work where HX had an effect beginning only 1-2 weeks after the injury, contusion or compression produces a virtually immediate deficit in conduction which can display some recovery. These discrepancies probably reflect the differences in the injury which in the case of contusion or compression involves virtually the entire cord unlike HX where the initial damage is more limited. However, the conduction studies described here indicate that deficits spread

across the cord from the HX and also to segments below. Such changes might also occur after contusion or compression, but would be obscured by the changes observed immediately after injury.

The threshold and conduction velocity of the volleys recorded here indicates that only the largest myelinated fibers were being monitored in these experiments. We can say little about smaller fibers, which may not have been affected to the same extent. Indeed, clinical observations such as preservation of somatosensation associated with the Brown Sequard syndrome indicate that numerous fibers contralateral to a hemisection are able to conduct through this region.

The mechanisms underlying the changes in conduction observed here are not clear at present. Our results suggest that fibers are present in VLF contralateral to the HX as observed by neurofilament labeling (Supplementary Fig. 1) and quantification of axonal profiles (Fig. 4). Although some decline in the number of VLF axons as well as demyelination was observed in the contralateral white matter with a time course consistent with the electrophysiological changes measured here, the reduction in the number of myelinated axons (about 40%) was not sufficiently great to account for the profound loss of the shortest latency electrophysiological responses which are due to volleys in myelinated fibers. This suggests that the surviving fibers had other deficits, e.g., in transmembrane ionic gradients or in Na channel function as has been suggested for the decline in conduction following compression injuries (36, 37). This could lead to conduction blocks or a decline in conduction velocity which would desynchronize the action potential volleys making them more difficult to detect. The decreased synaptic response may

have been due additionally to diminished synaptic transmission on target cells as has been observed for spinal synapses of afferent fibers that have been transected (38, 39).

Consistent with our electrophysiological findings at the cellular level, recent extracellular recordings from the lumbar epidural space have revealed the loss of waves of evoked potentials throughout the chronic lateral HX at the thoracic spinal cord (40). In another study, a combination of dorsal and lateral hemisection has been found to result in significantly lower amplitudes of electromyographic (EMG) responses from the triceps muscles following magnetic stimulation of the contralateral hip (41).

Interestingly, the 2-week time point, with the complete decline of transmission through the contralateral VLF, marked the end of spontaneous locomotor recovery of hindlimb function (Fig. 5). Numerous additional studies have shown that spontaneous recovery of hindlimb function and locomotor recovery ends 2 weeks after lateral HX (16-18, 40). Anatomical and behavioral studies indicate that the degree of locomotor recovery following a lesion of the spinal cord is directly correlated with the number of fibers remaining in the ventrolateral spinal cord, thus pointing to the role of these fibers in motor function (42). Robust spontaneous locomotor recovery during the first two weeks post lateral HX has been attributed to recovery from the initial spinal shock and enhanced anatomical plasticity of propriospinal/reticulospinal relay connections (17, 18, 43). The importance of these anatomical projections in determining the extent of recovery after HX adds significance to the present results. Here we show an association between the loss of functionality of the ipsilateral and contralateral projections in the white

matter through the segment of the HX and the sustained deficits in locomotor function of both hindlimbs while performing challenging behavioral tasks (Fig. 5).

In conclusion, this study is the first demonstration of the delayed decline of transmission through surviving descending axons to individual lumbar MNs induced by chronic incomplete spinal cord injury in adult rats. These findings may be useful experimentally since they provide a readily measured end point to evaluate strategies to minimize secondary effects of injuries.

Also, since clinical correlations in spinal cord-injured patients have demonstrated the validity of the rodent model for the study of neurological dysfunction after acute and chronic injuries (reviewed in 5, 11), our results suggest that in order to minimize and/or reverse developing conduction deficits, an appropriate treatment to minimize disruption of functional transmission by fibers surviving the injury should be introduced as soon as possible after the initial injury.

Figure Legends:

Fig. 1 Chronic injury, but not acute injury, induces decay of transmission to motoneurons through white matter contralateral to HX. Intracellular recordings were made *in vivo* from L5 motoneurons below the hemisection, in response to stimulation of ipsilateral and contralateral VLF at T6 above the level of injury. a-c: Responses from (A) ipsilateral and (B) contralateral VLF rostral to HX, and (C) ipsilateral VLF caudal to HX. Records displayed are among the largest responses for each group (average of 50 consecutive traces), with the arrow indicating the stimulus artifact at the left. Insets: superimposed 10 responses from same cell evoked by stimulation of the ipsilateral and contralateral VLF, respectively. Conditions: (i) intact spinal cord, (ii) same cord as above, but 10 minutes after HX, (iii) different cord, 4 wks post-HX. D: Position of the recording and stimulating electrodes. E: Reconstruction of the injury from T10 cross-sections from the cord presented in (iii); reconstruction from 3 sections 50 μ M apart superimposed onto templates modified from (44). F: Summary of results demonstrating the decline in magnitude of motoneurons responses in L5 ipsilateral to HX at T10 (stimuli were delivered at T6 ipsilateral and contralateral to the HX, and at L1 ipsilateral to the HX; the symbols above some of the bars represent a significant decline from controls ($p < 0.05$); all means were derived from $n = 5-9$ rats, and for each rat the response was an average of the maximum responses recorded intracellularly from 5 to 7 motoneurons).

Fig. 2. Extracellular responses in L5 ventral horn contralateral to HX elicited by stimulation at T6 contralateral to HX. Diagrams show positions of the recording tungsten electrode (right-side ventral horn) and the stimulating electrode (right side VLF), stimulus intensities (at 1 Hz stimulation rate) and the HX on the left side at T10. All superimposed traces are the successive

responses evoked by stimuli of opposite polarity (50 consecutive traces each polarity). a: Representative traces recorded in the intact cord. b: Lesion of the left side of the cord did not induce marked changes of the evoked potentials conducted through the right uninjured side across from HX. c: Lesion of half of the right side of the cord in addition to complete lesion of the left side resulted in smaller amplitude responses. d: Complete transaction of the cord (both left and right sides) completely abolished evoked responses, even at higher stimulus intensity.

Fig. 3. Intracellular and extracellular recordings demonstrating conduction deficit and decay of transmission contralateral to chronic HX. Diagrams show position of recording intracellular (clear arrow) and extracellular (solid arrow) stimulating electrodes, and stimulus intensity required to evoke responses in uninjured and chronically injured spinal cords. a1: intact spinal cord. Stimulation of right VLF at T6 elicits EPSP in an L5 motoneuron on the same side that is similar in amplitude and of longer latency than the response elicited in the same motoneuron by stimulation at L1. a2, b2: chronic left hemisected spinal cord. Intracellular and extracellular responses at right L5 ventral horn elicited by stimulation of right VLF at T6 (a2, b2) are considerably smaller than the responses elicited at the same electrodes by stimulation at L1 (a3, b3).

Fig. 4. Analysis of the total and myelinated axon number in the spared white matter on the intact side. A and B: Representative 60x (a) and Electron Microscope (b) images of the white matter (from labeled area in the insets). C: Number of myelinated axons in the spared white matter across from HX. Note marked decrease in the number of central myelinated axons in the spared

white matter on the intact side in chronic (2 weeks and 6 weeks post-HX) vs acute HX rats ($p < 0.05$, one way non-parametric ANOVA).

Fig. 5. Spontaneous recovery of locomotor function of both ipsilateral and contralateral to HX hindlimbs plateaus at about 2 weeks post-HX. In addition to BBB open-field locomotion score, we used more challenging tests, e.g. Narrowing Beam and Horizontal Irregular Ladder, to assess hindlimbs function ipsilateral and contralateral to the lesion. Values represent means \pm SEM with $p < 0.05$ for all values at post-HX time points vs pre-operation values. BBB-scoring during 1st week post-HX revealed that all rats start with a very similar handicap (lesion severity). Note that function recovers spontaneously, up to day 14 in all three tests, and after that recovery plateaus.

Supplementary Fig. 1. Neurofilament (NF-H, red) immunofluorescence demonstrating axonal sparing in white matter across the HX after acute and chronic HX, respectively. Representative images captured from horizontal sections at layer 7 level (close to midline) at areas labeled as A1 (HX on the left) and A2 (across from the HX, on the right). Scale bar is 100 μ m. Images were pseudo-colored in Photoshop.

REFERENCES

1. Bunge, R.P., Puckett W.R. & Hiester ED. Observations on the pathology of several types of human spinal cord injury, with emphasis on the astrocyte response to penetrating injuries. *Adv Neurol.* **72**, 305-15 (1997).
2. Burns, S.P., Golding, D.G., Rolle, W.A. Jr., Graziani, V. & Ditunno, J.F. Jr. Recovery of ambulation in motor-incomplete tetraplegia. *Arch Phys Med Rehabil.* **78**, 1169-72 (1997).
3. Little, J.W., Ditunno, J.F. Jr., Stiens, S.A. & Harris R.M. Incomplete spinal cord injury: neuronal mechanisms of motor recovery and hyperreflexia. *Arch Phys Med Rehabil.* **80**, 587-99 (1999).
4. Raineteau, O. & Schwab, M.E. Plasticity of motor systems after incomplete spinal cord injury. *Nat. Rev. Neurosci.* **2**, 263-73 (2001).
5. Gramsbergen A. Normal and abnormal development of motor behavior: lessons from experiments in rats. *Neural Plast.* **8**, 17-29 (2001).
6. Shefchyk, S.J. Spinal mechanisms contributing to urethral striated sphincter control during continence and micturition: "how good things might go bad". *Prog Brain Res.* **152**, 85-95 (2006).
7. Mayer, N.H. & Esquenazi, A. Muscle overactivity and movement dysfunction in the upper motoneuron syndrome. *Phys Med Rehabil Clin N Am.* **14**, 855-83 (2003).

8. Schallert, T. & Woodlee, M.T. Brain-dependent movements and cerebral-spinal connections: key targets of cellular and behavioral enrichment in CNS injury models. *J Rehabil Res Dev.* **40**, 9-17 (2003).

9. Yukawa, Y. *et al.* Postoperative changes in spinal cord signal intensity in patients with cervical compression myelopathy: comparison between preoperative and postoperative magnetic resonance images. *J Neurosurg Spine.* **8**, 524-8 (2008).

10. Jankowska, E. & Edgley, S.A. How can corticospinal tract neurons contribute to ipsilateral movements? A question with implications for recovery of motor functions. *Neuroscientist.* **12**, 67-79 (2006).

11. Johnson, R.D. Descending pathways modulating the spinal circuitry for ejaculation: effects of chronic spinal cord injury. *Prog Brain Res.* **152**, 415-26 (2006).

12. Arvanian, V.L., Schnell, L., Horner, P.J., Bowers, W.J., Federoff, H.J., Schwab, M.E. & Mendell LM. Combinatory treatment with Neurotrophin NT-3 secreting from fibroblasts, virally delivered NMDA-2D subunits and anti-nogo-a antibody (11c7, via osmotic minipump) induce reappearance and strengthening of multisynaptic connections in hemisectioned spinal cord in adult rats. SFN Abstract (2006).

13. Lou, L., Garcia-Alias, G., Mendell, L.M., Fawcett, J.W. & Arvanian, V.L. Transmission through white matter contralateral to thoracic hemisection declines beginning several days after injury in parallel with enhanced expression of CSPGs in the vicinity of the lesion. SFN Abstract (2007).
14. Golshani, R., Pearse, D.D., Lou, L., Mendell, L.M. & Arvanian, V.L. Decline of transmission to motoneurons from surviving fibers induced by chronic spinal cord hemisection in adult rats. SFN Abstract (2008).
15. Basso, D.M., Beattie, M.S. & Bresnahan, J.C. A sensitive and reliable locomotor rating scale for open field testing in rats. *Journal of Neurotrauma* **12**, 1-21 (1995).
16. Webb AA, Muir GD. Course of motor recovery following ventrolateral spinal cord injury in the rat. *Behav Brain Res.* **155**, 55-65 (2004).
17. Ballermann, M. & Fouad, K. Spontaneous locomotor recovery in spinal cord injured rats is accompanied by anatomical plasticity of reticulospinal fibers. *Eur J Neurosci.* **23**, 1988-96 (2006).
18. Courtine, G. *et al.* Recovery of supraspinal control of stepping via indirect propriospinal relay connections after spinal cord injury. *Nat Med.* **14**, 69-74 (2008).

19. Shumsky, J.S. et al. Delayed transplantation of fibroblasts genetically modified to secrete BDNF and NT-3 into a spinal cord injury site is associated with limited recovery of function. *Exp Neurol.* **184**, 114-30 (2003).
20. Liebscher, T. et al. Nogo-A antibody improves regeneration and locomotion of spinal cord-injured rats. *Ann Neurol.* **58**, 706-19 (2005).
21. Arvanian, V.L. et al. Combined delivery of neurotrophin-3 and NMDA receptors 2D subunit strengthens synaptic transmission in contused and staggered double hemisectioned spinal cord of neonatal rat. *Exp Neurol.* **197**, 347-52 (2006).
22. Shaw, G. et al. Hyperphosphorylated neurofilament NF-H is a serum biomarker of axonal injury. *Biochem Biophys Res Commun.* **336**, 1268-77 (2005).
23. McTigue, D.M., Tripathi, R. & Wei, P. NG2 colocalizes with axons and is expressed by a mixed cell population in spinal cord lesions. *J Neuropathol Exp Neurol.* **65**, 406-20 (2006).
24. Pearse, D.D. et al. Histopathological and behavioral characterization of a novel cervical spinal cord displacement contusion injury in the rat. *J Neurotrauma.* **22**, 680-702 (2005).
25. Fouad, K. et al. Combining Schwann cell bridges and olfactory-ensheathing glia grafts with chondroitinase promotes locomotor recovery after complete transection of the spinal cord. *J Neurosci.* **25**, 1169-78 (2005).

26. Jankowska, E., Hammar, I., Slawinska, U., Maleszak, K. & Edgley, S.A. Neuronal basis of crossed actions from the reticular formation on feline hindlimb motoneurons. *J Neurosci.* **23**, 1867-78 (2003).
27. Reed, W.R., Shum-Siu, A., Onifer, S.M. & Magnuson, D.S. Inter-enlargement pathways in the ventrolateral funiculus of the adult rat spinal cord. *Neuroscience.* **142**:1195-207 (2006).
28. Reed, W.R., Shum-Siu, A. & Magnuson, D.S. Reticulospinal pathways in the ventrolateral funiculus with terminations in the cervical and lumbar enlargements of the adult rat spinal cord. *Neuroscience.* **151**, 505-17 (2008).
29. Petruska, J.C. *et al.* Changes in motoneuron properties and synaptic inputs related to step training after spinal cord transection in rats. *J Neurosci.* **27**, 4460-71 (2007).
30. Hagg, T. & Oudega, M. Degenerative and spontaneous regenerative processes after spinal cord injury. *J Neurotrauma.* **23**, 264-80 (2006).
31. Donnelly, D.J. & Popovich, P.G. Inflammation and its role in neuroprotection, axonal regeneration and functional recovery after spinal cord injury. *Exp Neurol.* **209**, 378-88 (2008).

32. Kapoor, R, Davies, M & Smith, K.J. Temporary axonal conduction block and axonal loss in inflammatory neurological disease. A potential role for nitric oxide? *Ann N Y Acad Sci.* **893**,304-8 (1999)
33. Blight, A.R. Axonal physiology of chronic spinal cord injury in the cat: intracellular recording in vitro. *Neuroscience.* **10**, 1471-86 (1983).
34. Felts, P.A., Baker, T.A. & Smith, K.J. Conduction in segmentally demyelinated mammalian central axons. *J Neurosci.* **17**, 7267-77 (1997).
35. Nashmi, R. & Fehlings, M.G. Changes in axonal physiology and morphology after chronic compressive injury of the rat thoracic spinal cord. *Neuroscience.***104**, 235-51 (2001).
36. Shi, R. & Blight, A.R. Compression injury of mammalian spinal cord in vitro and the dynamics of action potential conduction failure. *J Neurophysiol.* **76**, 1572-80 (1996).
37. Schwartz, G. & Fehlings, M.G. Evaluation of the neuroprotective effects of sodium channel blockers after spinal cord injury: improved behavioral and neuroanatomical recovery with riluzole. *J Neurosurg.* **94**, 245-56 (2001).
38. Eccles, J.C., Krnjevic, K. & Miledi, R. Delayed effects of peripheral severance of afferent nerve fibres on the efficacy of their central synapses. *J Physiol.* **145**, 204-20 (1959).

39. Mendell, L.M., Taylor, J.S., Johnson, R.D. & Munson, J.B. Rescue of motoneuron and muscle afferent function in cats by regeneration into skin. II. Ia-motoneuron synapse. *J Neurophysiol.* **73**, 662-73 (1995).
40. Park, J.P. *et al.* Simple measurement of spinal cord evoked potential: a valuable data source in the rat spinal cord injury model. *J Clin Neurosci.* **14**, 1099-105 (2007).
41. Beaumont, E., Onifer, S.M., Reed, W.R. & Magnuson, D.S. Magnetically evoked inter-enlargement response: an assessment of ascending propriospinal fibers following spinal cord injury. *Exp Neurol.* **201**, 428-40 (2006).
42. You, S.W. *et al.* Spontaneous recovery of locomotion induced by remaining fibers after spinal cord transection in adult rats. *Restor Neurol Neurosci.* **21**, 39-45 (2003).
43. Bareyre, F.M. *et al.* The injured spinal cord spontaneously forms a new intraspinal circuit in adult rats. *Nat Neurosci.* **7**, 269-77 (2004).
44. Paxinos, G. Watson, C., Pennisi, M. & Toppole, A. Bregma, lambda and the interaural midpoint in stereotaxic surgery with rats of different sex, strain and weight. *J Neurosci Methods.* **13**, 139-43 (1985).

Acknowledgements: We thank Ms. Maria Amella, Ms. Katherine Leisha, Ms. Lauren Callier and Mr. Alex Tolpygo for technical support, Dr. Thomas Zimmerman and his staff for extensive veterinarian support, as well as Ms. Raisa Puzis and Ms. Margaret Bates of the electron microscopy core facility and finally Mr. Amitbhai S. Patel for his help with microscopy image analysis. This study was supported by grants from the Christopher Reeve Paralysis Foundation, NIH, NINDS and the NY State Spinal Cord Injury Foundation.

Author contribution:

VLA, LMM, LS, DDP, MES and JWF designed the experiments; VLA, LS, LL, RG and AH performed the experiments; VLA, LMM, JKR, LS, RG, AG, DDP, MES and JWF analyzed the data; VLA and LMM wrote the paper.

Table 1

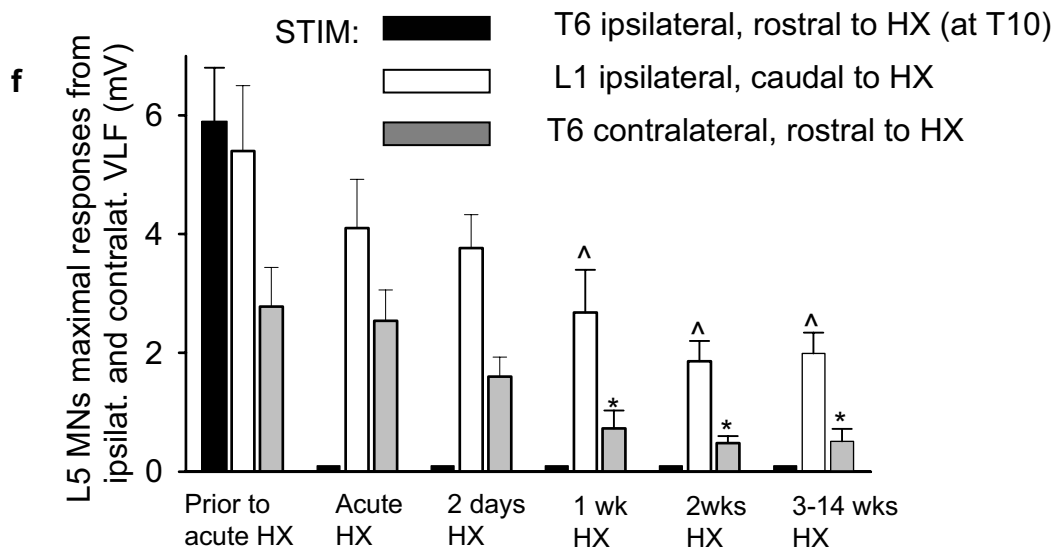
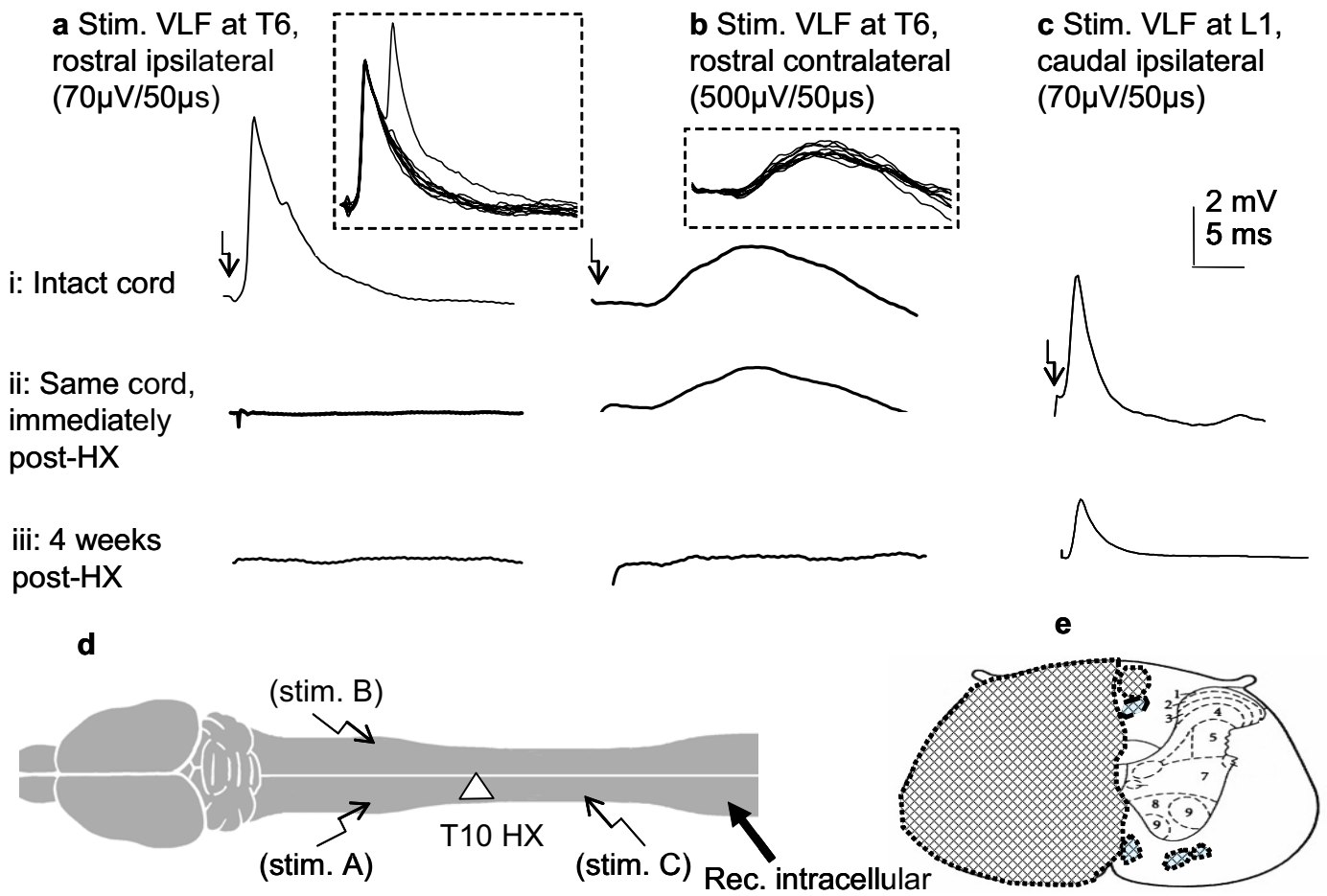
| Conditions | Stimulus location | Stimulus intensity (threshold) (μ A) | Stimulus intensity (max. response) (μ A) | Maximum synaptic response amplitude (mV) | Maximum volley amplitude (mV) |
|--|-------------------|---|---|--|-------------------------------|
| Intact (n=7) | Right VLF at T6 | 32 \pm 13 | 85 \pm 27 | 0.7 \pm 0.2 | 1.2 \pm 0.5 |
| Immediately after left HX at T10 (n=6) | Right VLF at T6 | 34 \pm 13 | 92 \pm 25 | 0.6 \pm 0.2 | 1 \pm 0.4 |
| 2+ weeks after left HX at T10 (n=11) | Right VLF at T6 | 250 \pm 36 * | 535 \pm 67 * | 0.09 \pm 0.04 * | 0.05 \pm 0.05 * |

Table 1: Extracellular recording of synaptic response at L5 in response to VLF stimulation at T6. Note that parameters immediately after HX are virtually unchanged from intact preparations. After chronic HX, required stimulus intensity is elevated (* $p < 0.05$) and amplitude of the maximum synaptic and volley responses are diminished (* $p < 0.05$).

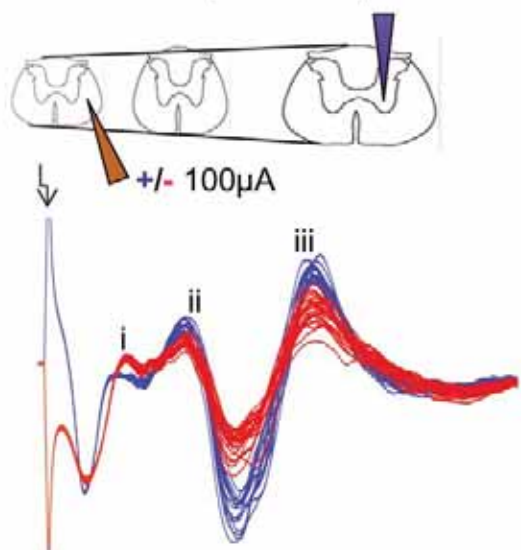
Table 2

| Preparation | Stimulus location | Stimulus intensity (max. response) (μA) | Maximum response amplitude (mV) | Latency (ms) |
|--------------------|--------------------------|---|--|---------------------|
| Intact (n=5) | Right VLF (T6) | 76 \pm 15 | 5.1 \pm 0.8 | 1.3 \pm 0.2 |
| Chronic HX (n=7) | Right VLF (T6) | 514 \pm 54 * | 0.9 \pm 0.2 * | 1.8 \pm 0.2 * |
| Intact (n=5) | Right VLF (L1) | 59 \pm 9 | 4.5 \pm 0.7 | 0.8 \pm 0.1 |
| Chronic HX (n=7) | Right VLF (L1) | 65 \pm 7 | 2.5 \pm 0.6 | 0.9 \pm 0.6 |

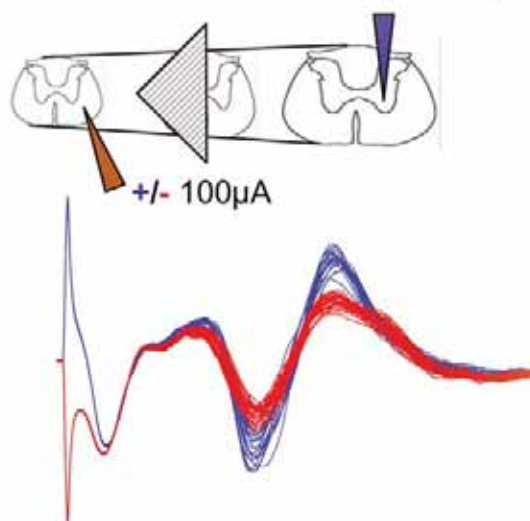
Table 2: Intracellular recording from motoneurons at L5 (right side of spinal cord) in response to stimulation of VLF at T6 and L1. Intact and chronic HX of left cord at T10. Note the difference between the responses elicited above the level of HX in intact and chronic HX cords (reduced response amplitude, increased latency, increased stimulus current required). Note the similarity in the parameters in intact and injured cord when stimulation was at VLF below the HX.



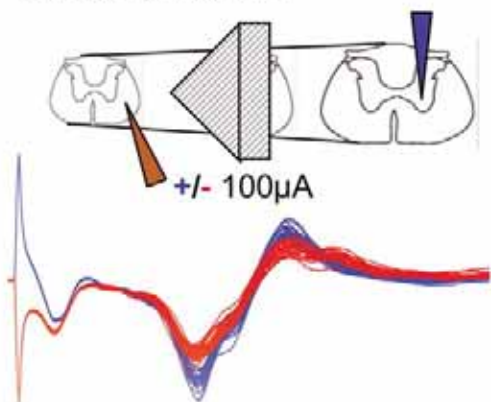
a: Control (intact cord)



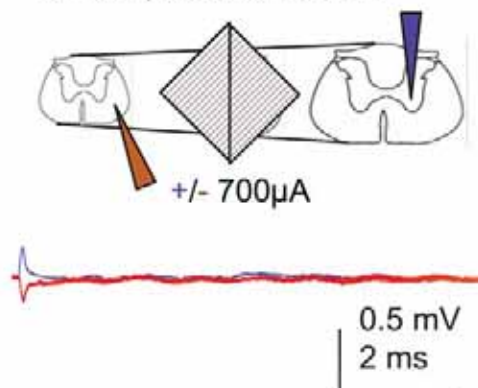
b: 5 min post-Hemisection (at T10)

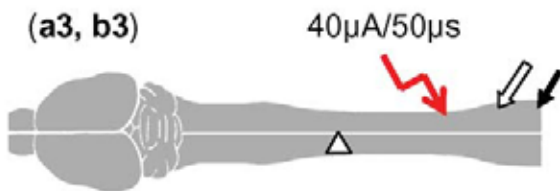
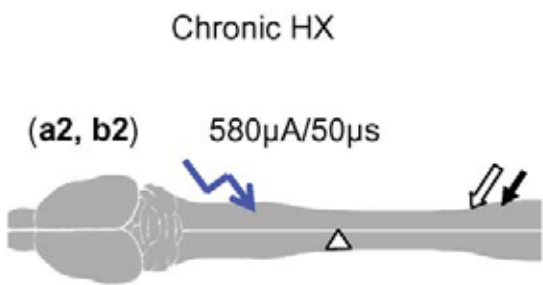
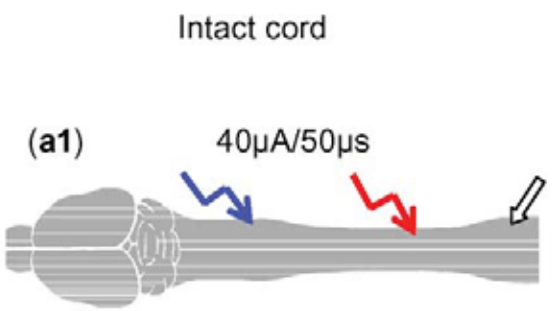


c: Overhemisection

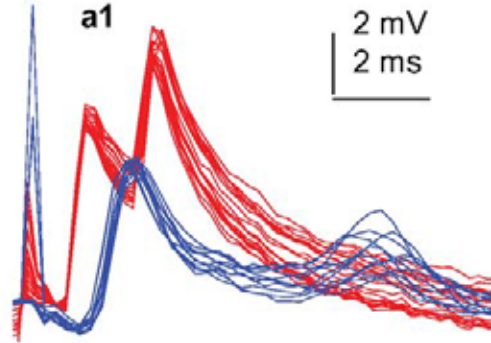


d: Complete transection

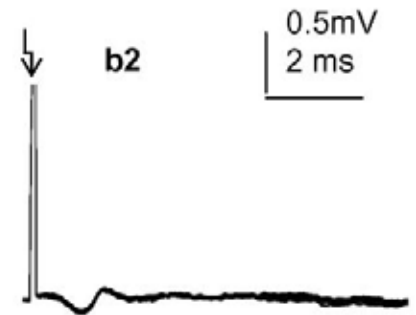




a: Intracellular recordings



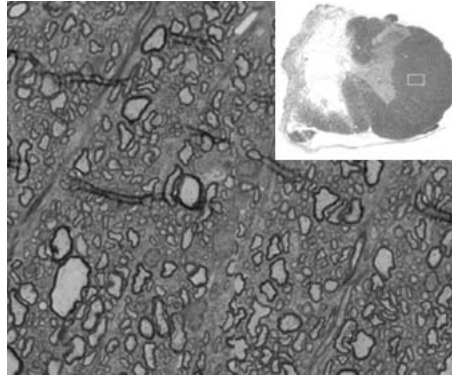
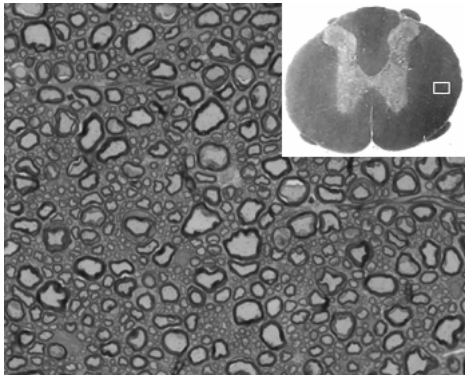
b: Extracellular recordings



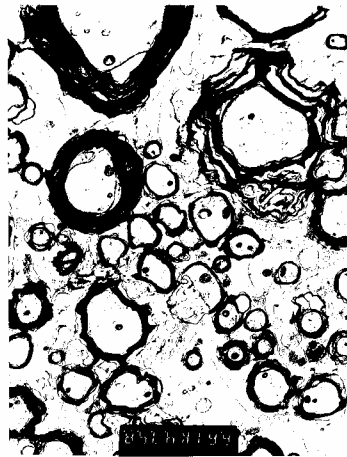
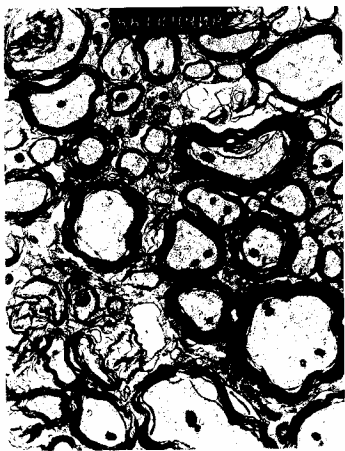
T10, non-injured

T10, 6 wks post-HX

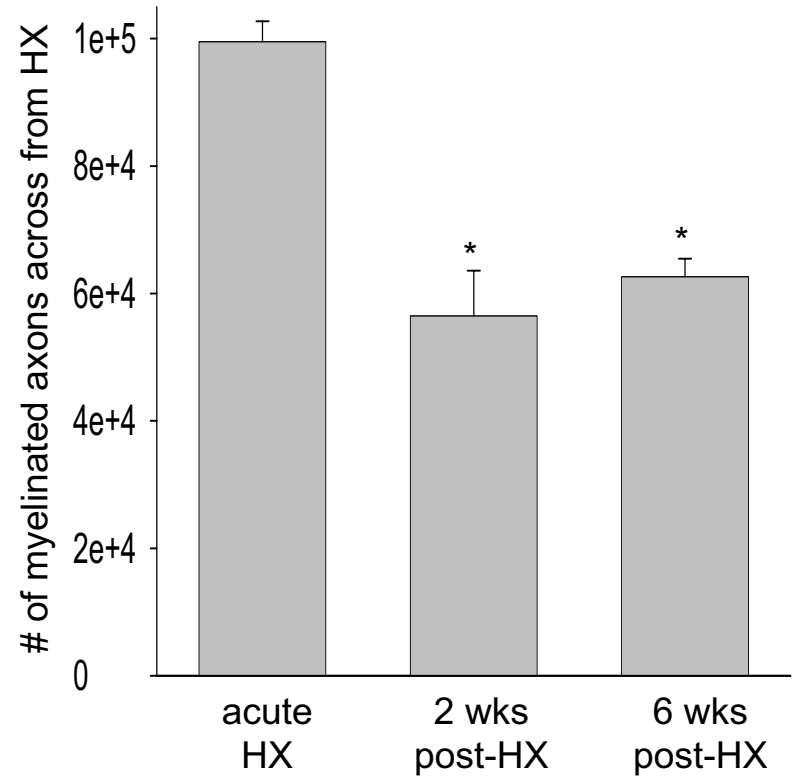
a



b



c



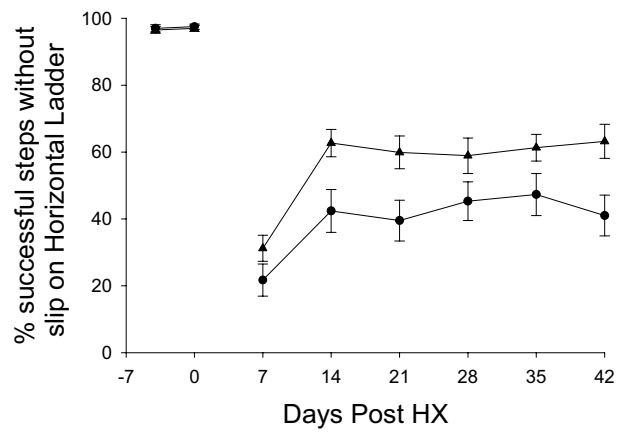
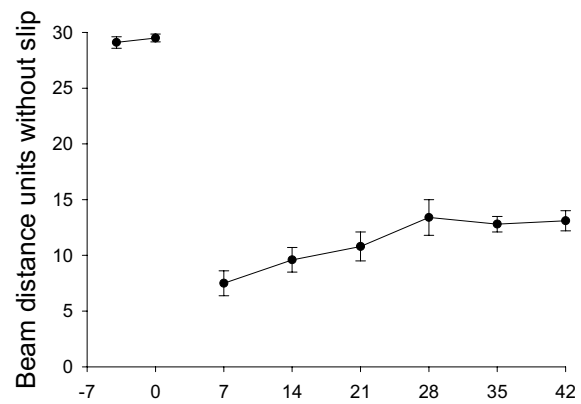
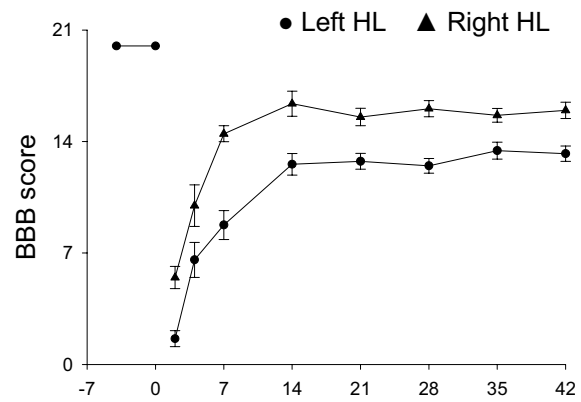


Table 1 Arvanian

| Conditions | Stimulus location | Stimulus intensity (threshold) (μ A) | Stimulus intensity (max. response) (μ A) | Maximum synaptic response amplitude (mV) | Maximum volley amplitude (mV) |
|--|-------------------|---|---|--|-------------------------------|
| Intact (n=7) | Right VLF at T6 | 32 \pm 13 | 85 \pm 27 | 0.7 \pm 0.2 | 1.2 \pm 0.5 |
| Immediately after left HX at T10 (n=6) | Right VLF at T6 | 34 \pm 13 | 92 \pm 25 | 0.6 \pm 0.2 | 1 \pm 0.4 |
| 2+ weeks after left HX at T10 (n=11) | Right VLF at T6 | 250 \pm 36 * | 535 \pm 67 * | 0.09 \pm 0.04 * | 0.05 \pm 0.05 * |

Table 1: Extracellular recording of synaptic response at L5 in response to VLF stimulation at T6. Note that parameters immediately after HX are virtually unchanged from intact preparations. After chronic HX, required stimulus intensity is elevated (* $p < 0.05$) and amplitude of the maximum synaptic and volley responses are diminished (* $p < 0.05$).

Table 2 Arvanian

| Preparation | Stimulus location | Stimulus intensity (max. response) (μ A) | Maximum response amplitude (mV) | Latency (ms) |
|------------------|-------------------|---|---------------------------------|-----------------|
| Intact (n=5) | Right VLF (T6) | 76 \pm 15 | 5.1 \pm 0.8 | 1.3 \pm 0.2 |
| Chronic HX (n=7) | Right VLF (T6) | 514 \pm 54 * | 0.9 \pm 0.2 * | 1.8 \pm 0.2 * |
| Intact (n=5) | Right VLF (L1) | 59 \pm 9 | 4.5 \pm 0.7 | 0.8 \pm 0.1 |
| Chronic HX (n=7) | Right VLF (L1) | 65 \pm 7 | 2.5 \pm 0.6 | 0.9 \pm 0.6 |

Table 2: Intracellular recording from motoneurons at L5 (right side of spinal cord) in response to stimulation of VLF at T6 and L1. Intact and chronic HX of left cord at T10. Note the difference between the responses elicited above the level of HX in intact and chronic HX cords (reduced response amplitude, increased latency, increased stimulus current required). Note the similarity in the parameters in intact and injured cord when stimulation was at VLF below the HX.